J. Appl. Environ. Biol. Sci., 5(10S)518-527, 2015

ISSN: 2090-4274
Journal of Applied Environmental and Biological Sciences
www.textroad.com

Discrete Element Modeling Tensile Fracture of Cemented Grout Specimens Reinforced by Short Polypropylene Fibers

A. Refahi[1], J. Aghazadeh Mohandesi[2]

[1]Assistant Professor, Department of Mining, Faculty of Engineering, University of Zanjan, Zanjan, Iran.
[2]Professor, Metallurgical Engineering Department, AmirKabir University of Technology, Tehran, Iran.

Received: April 20, 2015
Accepted: June 15, 2015

ABSTRACT

In this study, discrete element method (DEM) was used to model fracture energy and strength of cemented grout specimens reinforced by two morphologies of randomly distributed and parallel polypropylene short fibers along tensile direction. For this purpose, a standard-direct-tensile test was carried out on plan and reinforced specimens, and then the tests were simulated by DEM technique; in order to validate the models, the obtained results were compared by those experimentally evaluated. The results showed that the randomly distributed fibers had little effect on the tensile strength, however they enhanced remarkably the fracture energy of reinforced grouts. But, the fibers with the unidirectional orientation increased both the strength and fracture energy, which these results may be due to high absorbing energy in the fiber bridging zone.

KEYWORDS: Discrete element method; Tensile strength; Fiber reinforced cemented grout

1. INTRODUCTION

Short fibers have been widely used in concrete to improve its engineering properties and performances. These fibers include metals such as steel fibers, organic fibers and inorganic fibers. Polypropylene fibers are popular material used in the concrete industry because of their high modulus, high strength and excellent electrical properties. Polypropylene was the first synthetic stereo regular polymer to achieve industrial importance and it is presently the fastest growing fiber for technical end-uses where high tensile strength coupled with low-cost are essential features; it has shown consistent growth of about 5% per annum for the last 10 years [1, 2]. Researchers have reported that the polypropylene fibers can increase the flexural strength and ductility [3, 4], compressive and tensile strength [4, 5], toughness and modulus of rupture [4], and long-term durability of concretes [6]. Additionally, the fibers reduce the plastic shrinkage, improve permeability and are able to release the vapor pressure of concretes [7-9]. In this study, tensile fracture behavior of plain cemented grouts and reinforced cemented grout by short polypropylene fibers were modeled with discrete element method (DEM). DEM is a numerical technique for simulating dynamic and pseudo-static motions of interacting rigid bodies. The DEM was pioneered by Cundall to model the behavior of soil particles under dynamic loading [10]. Unlike other numerical methods that are based on continuum assumptions, the unique feature of the DEM allows us to model crack initiation and propagation in the context of the bonded-ball model [11,12]. This technique has been used successfully for modeling rock [13], concrete [14] and particular composite behavior [15].

In the present study, DEM technique was used to investigate fracture strength of cemented grout specimens reinforced by short polypropylene fibers. For this purpose, samples of plain specimens and reinforced grouts by two morphologies of randomly distributed and parallel polypropylene fibers were prepared, and then a standard-direct-tensile test was carried out on them. Subsequently, a DEM model of the tensile test was developed and the obtained results were compared by those experimentally estimated.

2. MATERIALS AND METHODS

The cemented grout specimens were produced by mixing 20 Kg of Conbextra BB80 grout (with 2300 Kg/m^3 density) complying with ASTM C1107 Grade C and 3 liters of water. Conbextra BB80 is an exceptionally high strength grout designed for grouting beneath bridge bearings, parapet posts and flanged lighting columns, heavy stanchion bases and base plates for reciprocating machines. The physical properties of this grout, which can be poured or pumped, are non-shrink, high early and ultimate compressive strength, good flow particularly at low temperature and low permeability ensures durability as shown in Table 1. In order to reinforce the cemented grout by randomly distributed fibers, monofilament polypropylene fibers with 12 mm length and 0.3 mm thickness were manually fibrillated (Fig. 1). It has been shown that the fibers with 12 mm length had the best performance for reinforcing cement grouts [16]. Then, 200 g grout

Corresponding author: A. Refahi, Assistant Professor, Department of Mining, Faculty of Engineering, University of Zanjan, Zanjan, Iran. Postal address: Department of Mining, Faculty of Engineering, University of Zanjan, Zanjan, Tabriz Road, Zanjan, Iran. Tel Number: +989123034360 E-mail address: refahi.arash@znu.ac.ir, refahi.arash@gmail.com

powder was mixed with 15 cc water for 5 minutes in a pan mixer while 1 g fibrillated polypropylene fibers were gradually added to it. Two samples were similarly produced and mixed together by means of the pan mixer for 5 minutes, and then the mixture was poured into a dog bone mold as shown in Fig. 2 (based on ASTM C190-85 standard). Since the polypropylene is hydrophobic and non-polar, the fibers were gradually introduced to the cemented grout. Referring to the fiber density (Table 2), the fiber volume fraction was equal to 1% that was in the range described in the previous work (i.e. 1-5%) [17]. To produce the unidirectional fiber reinforced grout, nine glass tubes with 1.2 mm inner diameter, 1.5 mm outer diameter and 100 mm length were placed in the mold in a square pattern with 7 mm apart (Fig. 3). 0.22 g fibers were located in each tube by pushing through a steel mandrel with 1 mm diameter. Subsequently, the wet grout was poured in the mold and the tubes were immediately brought out from the mold. In order to locate the fibers unidirectionally and evenly, the tubes were brought out with a constant speed while the steel mandrel was firmly fixed. To achieve the homogenous distribution of fibers, the procedure was repeated several times were by try and error until the best manual procedure was obtained. All specimens remained in the molds for 24 hours, and then those were brought out from the molds and cured in water for one week to complete the hydration reaction.

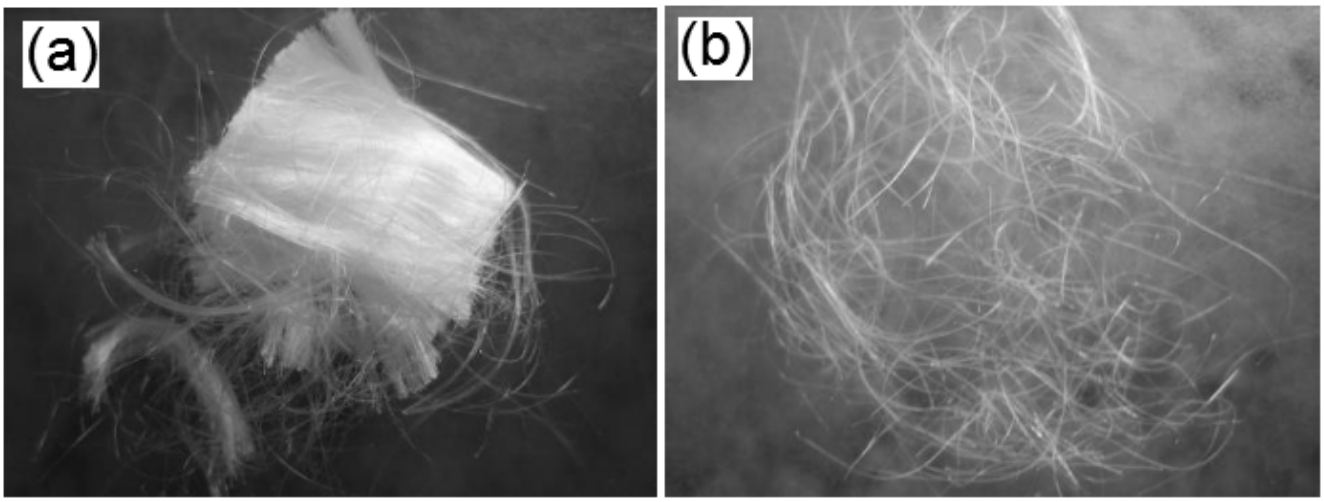

Fig. 1. a) Monofilament and b) fibrillated polypropylene fibers.

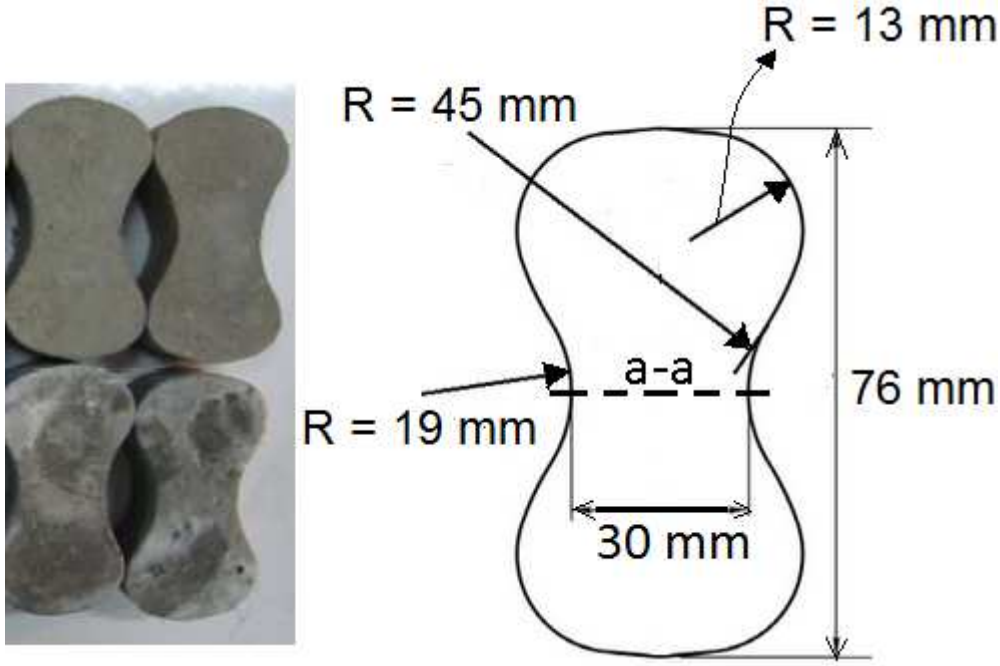

Fig. 2. Dog bone specimens of studied cemented grouts.

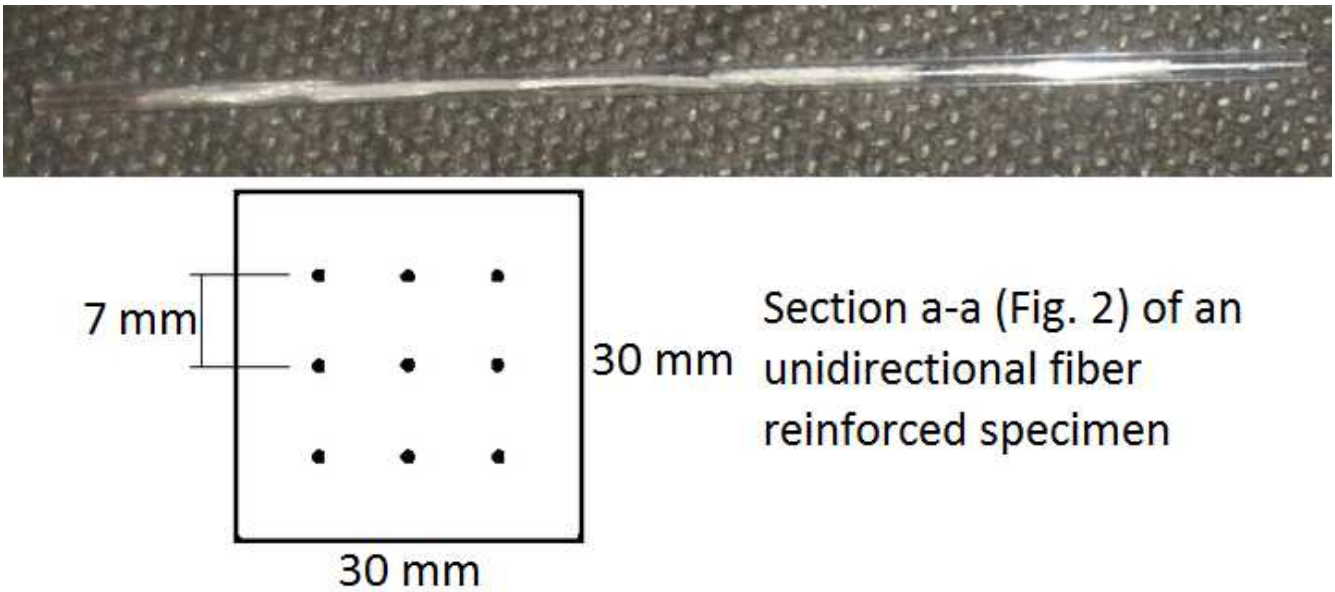

Fig. 3. A glass tube containing polypropylene fibers.

Test methods	Typical results
Compressive strength (BS 1881: part 116 1983)	45 MPa at 24 hours 60 MPa at 3 days 70 MPa at 7 days 90 MPa at 28 days
Expansion (ASTM C827-87)	Controlled positive expansion
Total chloride ion content	<0.1%
Rapid chloride permeability (AASHTO T277)	Very low
Water permeability (DIN 1048 Pt. 5:1991)	< 2 mm
Total acid soluble: sulphate SO_3	< 4%

Table 1. Physical and mechanical properties of mixing 20 Kg of Conbextra BB80 grout with 3 liter water at room temperature.

Property	Value
Elastic modulus	8.5 GPa
Tensile strength	580 MPa
Melting point	160º C
Density	910 Kg/m^3

Table. 2. Properties of polypropylene.

To determine tensile strength of the plain and reinforced cemented grout, a standard-direct-tensile test was carried out on the studied specimens. Some samples of each specimen were employed for the tensile test using a servo hydraulic Instron testing machine; the unidirectional fibers were along the tensile direction. The extension rate was 0.5 mm/min. In order to increase the accuracy of the results, only the results obtained from the specimens broken in the vicinity of the middle of specimen (Fig. 4) were recorded rather than those broken in the areas near the jaws to eliminate the effect of stress concentration impose by the jaws.

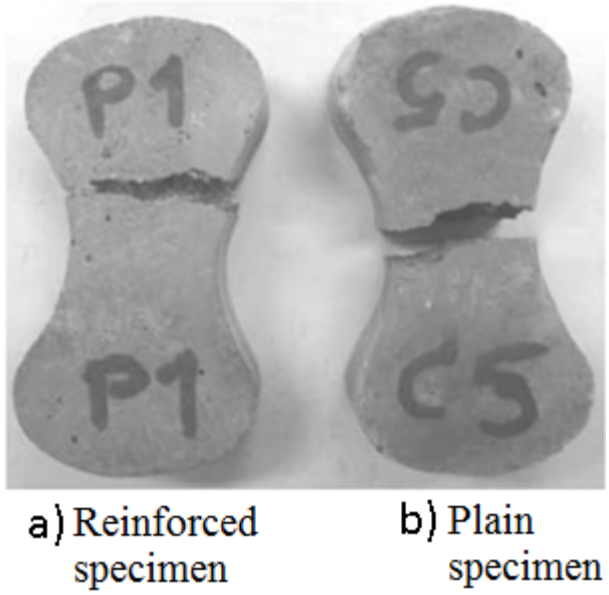

Fig. 4. Two cemented grout specimen broken in a) areas near the jaws b) vicinity of middle of specimen.

3. RESULTS AND DISCUSSION

The evaluated tensile strength and elastic modulus of the cemented grout specimens showed that the scatter of the results was very high; the measured tensile strength of specimens is given in Table 3. This is common for these specimens under tensile testing where the flaws vary in size, shape and orientation, causing the strength to vary from specimen to specimen [18]. Weibull statistical approach was used to determine the statistically most probable results. The basic assumption in Weibull distribution is that a body of a material has a statistical distribution of noninteracting fractures. If there are N broken specimens of a brittle material that were tested, the fracture probability of a specimen with number of i ($F_i(V)$) is equal to:

$$F_i(V) = i/(N+1) \tag{1}$$

Based on Weibull distribution, the fracture probability of each specimen can be related to the maximum applied stress (i.e. fracture strength $\sigma_{\max}$) during the test as follow:

$$1 - F(V) = \exp\left[\left(\sigma_{\max} / \sigma_0\right)^m\right] \tag{2}$$

Where σ_0 is a characteristic fracture strength of the material that it is often defined as the mean strength of it and m is the Weibull modulus measuring the variability of the evaluated data; the higher the value of m, the less is the material variability in the strength. A double-logarithmic plot of Eq. (2) will give a straight line with slope m as following expressed [18]:

$$\ln\left[\ln\left(1/(1-F(V))\right)\right] = m \ln \sigma_{\max} - m \ln \sigma_0 \tag{3}$$

Consequently, the mean strength and elastic modulus of the studied cemented grouts can be evaluated by passing the best line through the experimentally obtained data using the regression approach [19]; the obtained results are shown in Table 4. The effect of randomly distributed fibers on increasing the strength seems not considerable. It showed that in the reinforced concrete with a low to medium value of fiber volume fraction, the fibers did not remarkably enhance the strength of concrete and the benefits of the fiber reinforcement were limited to enhance absorbed energy or toughness in post-cracking region only. However, the unidirectional fibers enhanced the tensile strength of specimens. The cemented grout samples carry flaws and micro cracks both in the material and at the interfaces. Under an applied load, the distributed micro cracks propagate, coalesce and align themselves to produce macro cracks. When load are further increased, conditions of critical crack growth are attained at the tips of macro cracks and a catastrophic failure is precipitated. However, the fibers bridge the propagating cracks in the reinforced specimens because the grout failure precedes the fiber failure. This causes the fiber bridging zone to absorb a lot of energy by fiber debonding, fiber pullout (sliding) and fiber rupture when a crack propagates across a fiber through the grout as illustrated in Fig. 6. Consequently, the energy absorption capacity of the unidirectional fiber reinforced specimen increases and their cracking sensitivity decreases, causing the fracture strength to increase [20].

Number of specimen (i)	Fracture probability ($F(V)$)	Tensile strength MPa	Tensile strength MPa	
			Reinforced by randomly distributed fibers	Reinforced by unidirectional fibers
1	0.07	3.4	11.5	37.4
2	0.13	2.8	10.9	31.5
3	0.2	1.5	12.5	46.3
4	0.27	3.9	10.6	33
5	0.33	4.3	11.4	37.6
6	0.4	4.9	12.4	33.9
7	0.47	4.7	10.9	29.8
8	0.53	3	12.4	45.7
9	0.6	5.4	11.4	39.7
10	0.67	2.6	12.9	50.2
11	0.73	3.8	11	34.2
12	0.8	3.1	11.6	39.2
13	0.87	2.9	12.7	50.6
14	0.93	3.4	11	34.6

Table 3. Tensile strength of studied cemented grouts.

Cemented grout	Mean tensile strength MPa	Mean elastic modulus GPa
Plain grout	9.5	11.7
Reinforced grout by randomly distributed fibers	14	19.3
Reinforced grout by parallel fibers	52.8	35.6

Table 4. Mean tensile strength and elastic modulus of studied cemented grouts.

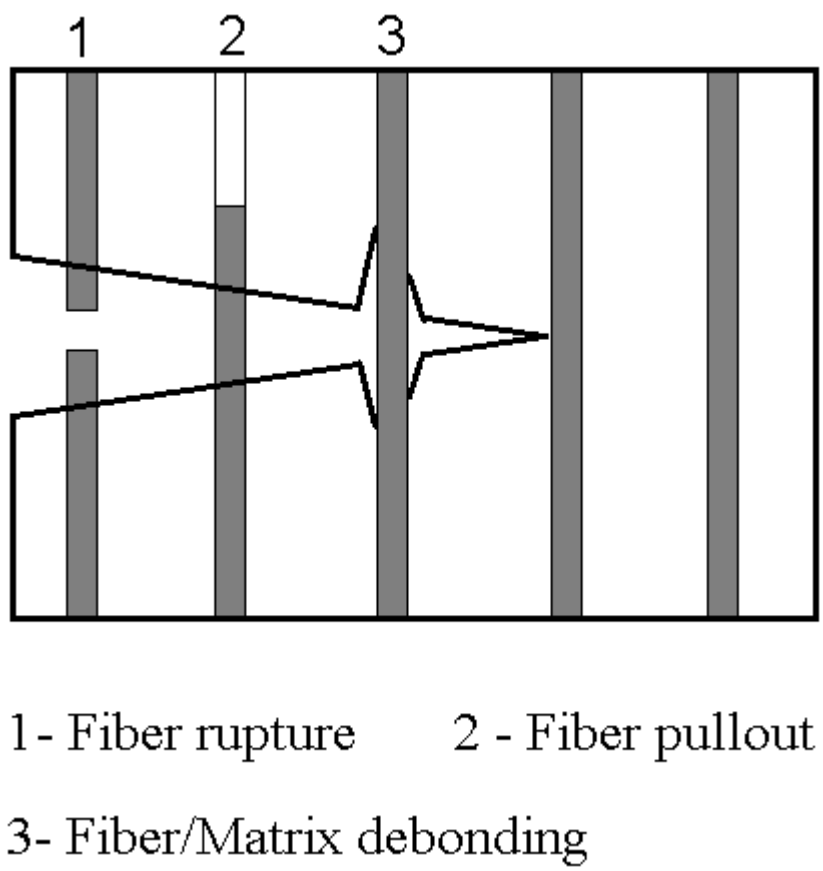

Fig. 6. Methods of absorbed energy in fiber bridging zone.

4. Discrete element method

In this study the plain and reinforced grouts were simulated by PFC3D software based on discrete element method (DEM). With DEM it is possible to model the behavior of rigid balls that may be enclosed within a finite volume by non-deformable walls. The code keeps a record of individual balls and updates any contact with other balls or walls. Each calculation step includes the solution of motion equations to a ball, using a force-displacement law for each contact. Also, the balls can be bonded together at the contact points that will be described. The contact stiffness between two balls is modeled as a set of elastic springs with a constant normal and shear stiffness as shown in Fig. 7. When two balls overlap, a normal and shear contact force develop at the contact point based on a force-displacement law, causing a relative motion to occur between two balls during each calculation step by solving equations of motion. The normal contact force (F^n) and shear contact force (F^s), expressed as following, are applied perpendicular and parallel to the contact surface, respectively:

$$F^n = K^n U^n$$
$$\Delta F^s = -K^s \Delta U^s \tag{4}$$

Where U^n and ΔU^s are the normal displacement and the increment of shear displacement between two balls, respectively. Also, K^n and K^s are the normal and shear contact stiffness, respectively. The assumed bond is created at the contact point between two balls and defined using a tensile and shear strength based on the force dimension (Fig. 7); this is called the contact bond. If either the maximum normal or shear force developed at a contact exceeds the corresponding bond strength, the bond will break and a micro crack will be created.

The micro parameters that are input to PFC3D software for modeling are the ball-ball contact modulus (E_b), the contact-bond normal strength (σ_n), the contact-bond shear strength (σ_s) and the ball density. The normal and shear contact strength based on the force dimension (F_n and F_s respectively) and the normal and shear contact stiffness between two balls are computed using following equation:

$$K^n = 4E_b\left((R_A + R_B)/2\right)$$
$$K^s = \alpha K^n$$
$$F^n = 4\sigma_n((R_A + R_B)/2)^2 \tag{5}$$
$$F^s = 4\sigma_s((R_A + R_B)/2)^2$$

Where α is the stiffness ratio (K^s / K^n). The computing method of contact stiffness between a ball and a wall is similar to that between two balls. However the contact bond is not created at the point contact between a ball and a wall [11, 12].

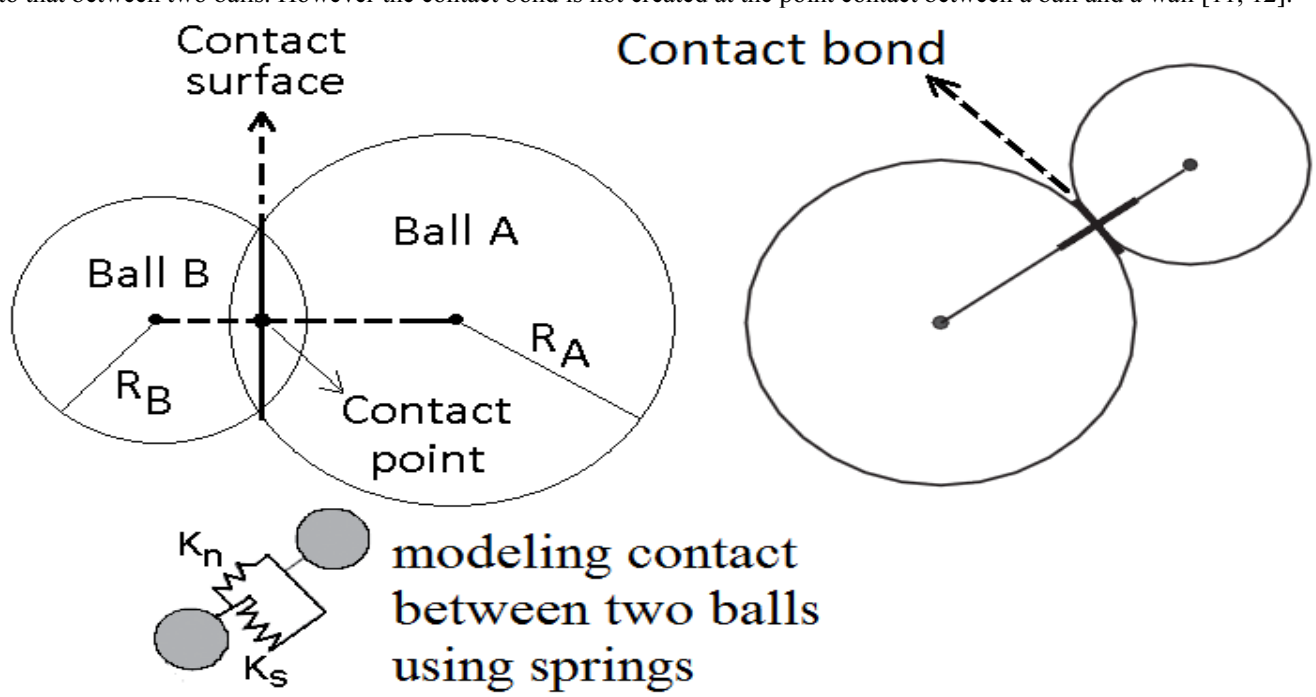

Fig. 7. Contact between two balls [21].

4.1. Discrete element model of cemented grout and polypropylene

PFC3D software simulates macro-scale material behavior from the interactions of micro-scale components; the input parameters are micromechanical properties of constituents. These micromechanical properties cannot be derived directly from measurements of laboratory specimens. To estimate properties of constituent balls and their bonding strength for modeling the cemented grout, the corresponding tensile test applied to it was simulated; the input micro parameters were changed by try and error until the calculated fracture strength matched that experimentally estimated. Consequently, a parallelepiped assembly of rigid balls bonded together was prepared from the cemented grout with 10*10*30 mm dimensions as shown in Fig. 8; the model was created using 17241 balls with diametric size distribution from 0.2 mm to 0.4 mm. Subsequently a thin layer of balls at the top and bottom of the specimen was identified and their velocity was fixed in the axial direction (Y direction). Consequently, the specimen was pulled apart slowly in Y direction while monitoring the axial force and axial displacement, which were converted to stress and strain by dividing by the specimen initial cross-sectional area and length, respectively. The pulling velocity was equal to 0.5 mm/min. If this velocity was applied in a single calculation step, the large acceleration produced inertial forces within the specimen that may produce damage. In order to eliminate such inertial effects, the velocity was adjusted to reach 0.5 mm/min in sequences of 100 steps. When the test was applied, the axial force (F) was monitored, and the maximum value was recorded ($F_{\max}$). During the test, F increased to a maximum point, and then decreased as the specimen failed and consequently the test was terminated when $|F| \leq 0.6|F_{\max}|$. The obtained stress-strain curve is shown in Fig. 8; the low value of consumed strain energy shows that a catastrophic failure may occur in the cement grout. Similarly, a DEM model of the polypropylene was developed and the tensile test was simulated accordingly. The obtained micromechanical properties of the grout and polypropylene are given in Table 5.

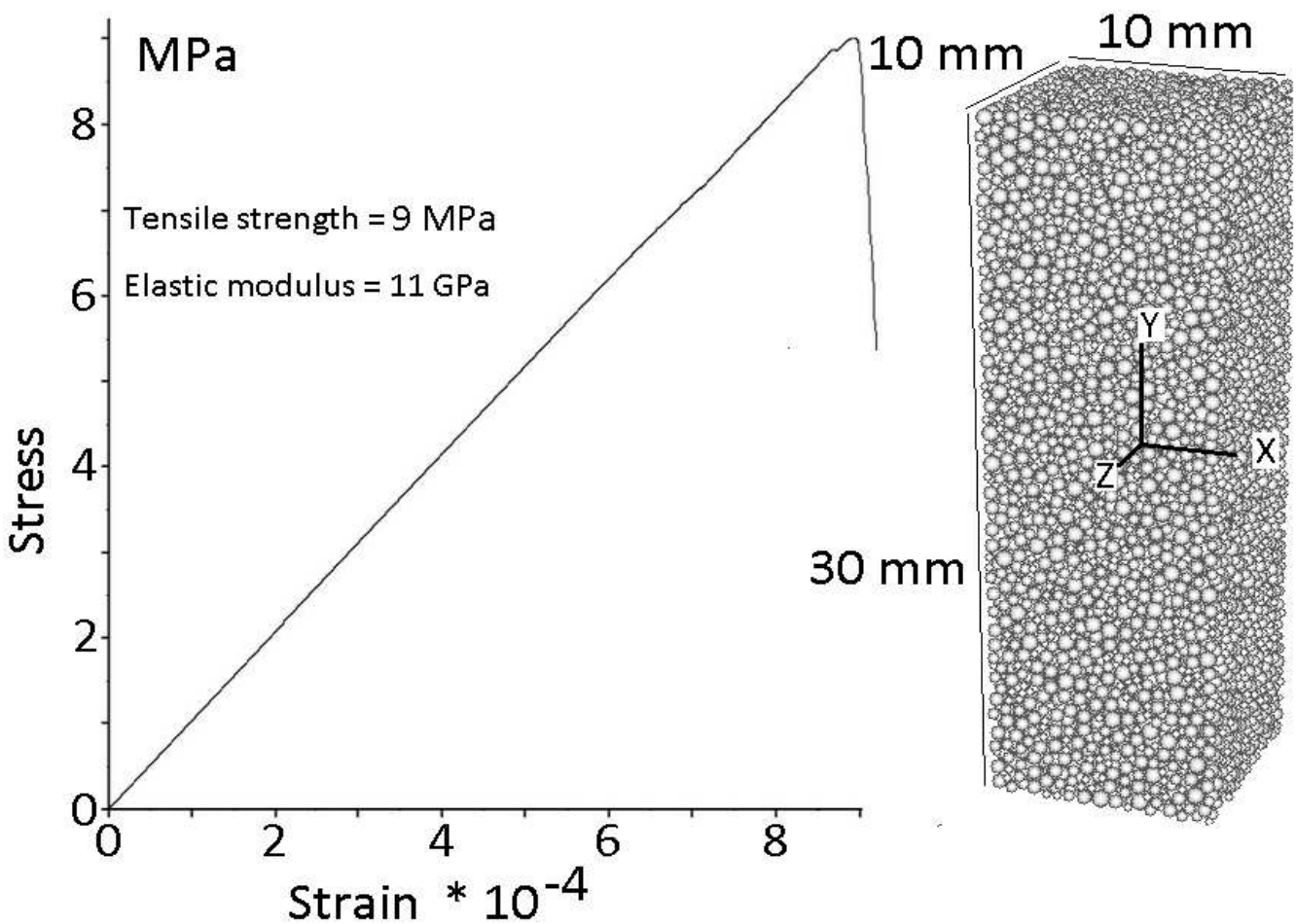

Fig. 8. DEM model of plain grout and obtained stress-strain curve.

Micromechanical properties	Polypropylene	Cemented grout
Ball–ball contact modulus (GPa)	8	12
Contact-bond normal strength (MPa)	880	6.4
Contact-bond shear strength (MPa)	880	6.4

Table 5. Micromechanical properties of plain cemented grout and polypropylene determined from DEM models.

4.2. DEM model of fiber reinforced cemented grout

In order to reduce errors in modeling the randomly distributed fiber reinforced grout, the minimum cross section of dog bone specimen has been divided to nine elements (i.e. element dimensions of 10*10 mm). Assuming 30 mm gauge length, the nine elements with different random orientation of fiber have been modeled. Accordingly, each element consists of 6 randomly distributed fibers containing forty closed packed balls as a string (i.e. similar fiber density of the laboratory specimen) as shown in Fig. 9. The micro properties of polypropylene modeled as string of balls (i.e. ball-ball contact) are given in Table 5, and the micro properties of contact between a ball in the fiber and that of grout were changed until the obtained fracture strength matched those experimentally evaluated; the estimated mean-normal and shear bond strength between fibers and grout were equal to 40 and 40 MPa, respectively. Subsequently, the tensile test was modeled similar to the plain grout, and the tensile strength was determined; the mean strength and elastic modulus were equal to 14.3 and 22 with the low deviation with the experimental mean data (Table 4). A typical stress-strain curve is shown in Fig. 9; similar to the previous works the effect of polypropylene fibers on increasing the fracture strength is not considerable. However, the reinforced specimen exhibits a non-linear increase of stress until the maximum, followed by gradual decrease in the stress which is a typical pseudo plasticity behavior. The higher strain energy of the reinforced grout is a typical progressive fracture behavior rather than a catastrophic one [22, 23].

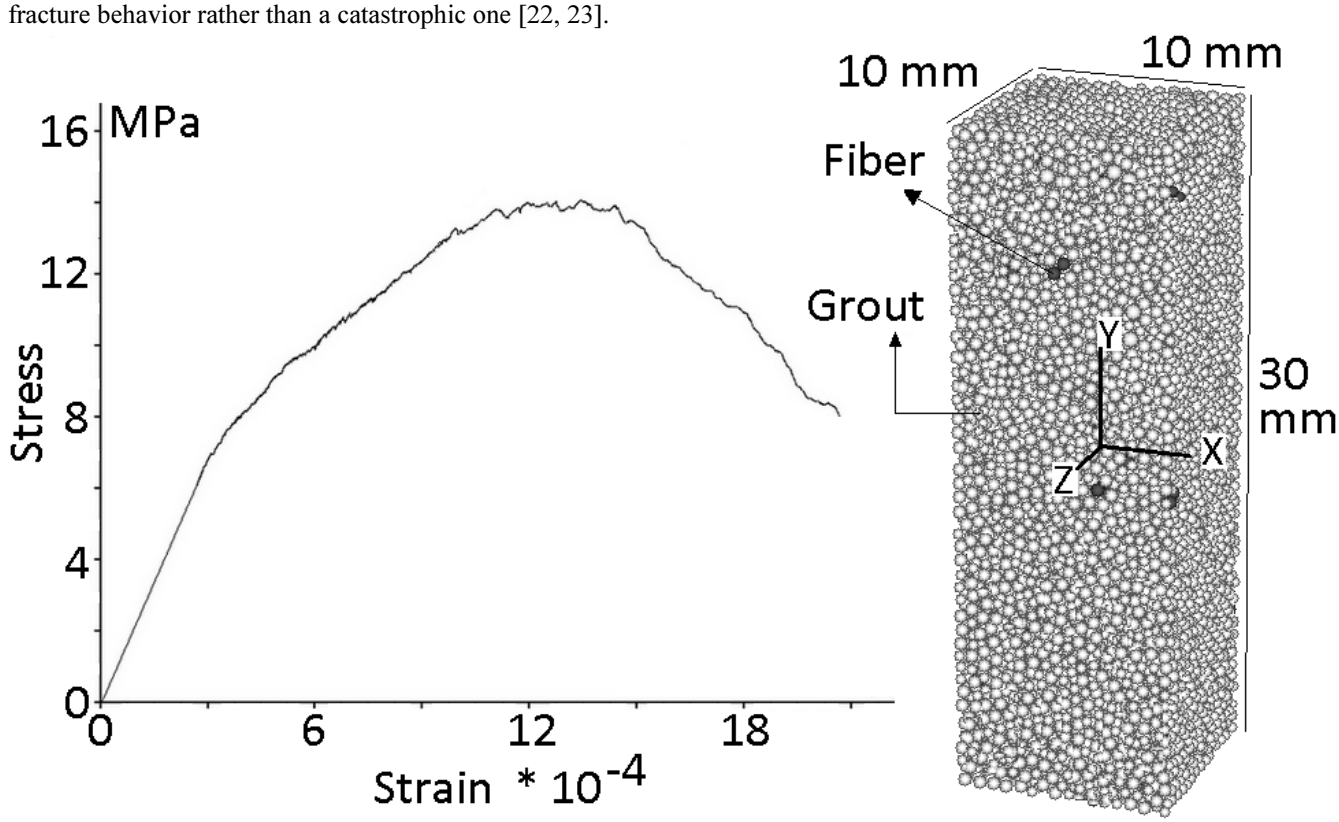

Fig. 9. One of PFC3D models of cemented grout reinforced by randomly distributed fibers and obtained stress-strain curve.

In order to model the unidirectional fiber reinforced grout, a parallelepiped model of the cemented grout with 10 mm sides and 30 mm high was developed and parallel fibers was generated in the grout as shown in Fig. 10. Similar to the section 4.1, the tensile test was modeled and fracture the stress-strain curve was determined as shown in Fig. 11; it seems that a noncatastrophic fracture occurs in the specimen. Unlike the randomly distributed fibers, the fracture strength of the reinforced cemented grout by the parallel fibers increases. These results may be due to high absorbed energy in the fiber pullout, fiber rupture and fiber debonding zone (i.e. the fiber bridging zone) when cracks propagate across the fibers through the cement grout. Therefore, the bridging zone consumes a lot of energy, causing the strength and strain energy of the specimen to increase and the reinforced grout to showing a pseudo plasticity behavior [22, 23]. Also, the determined strength that is close to the experimental data illustrates that the DEM is a suitable technique for simulating the polypropylene fiber reinforced cemented grout.

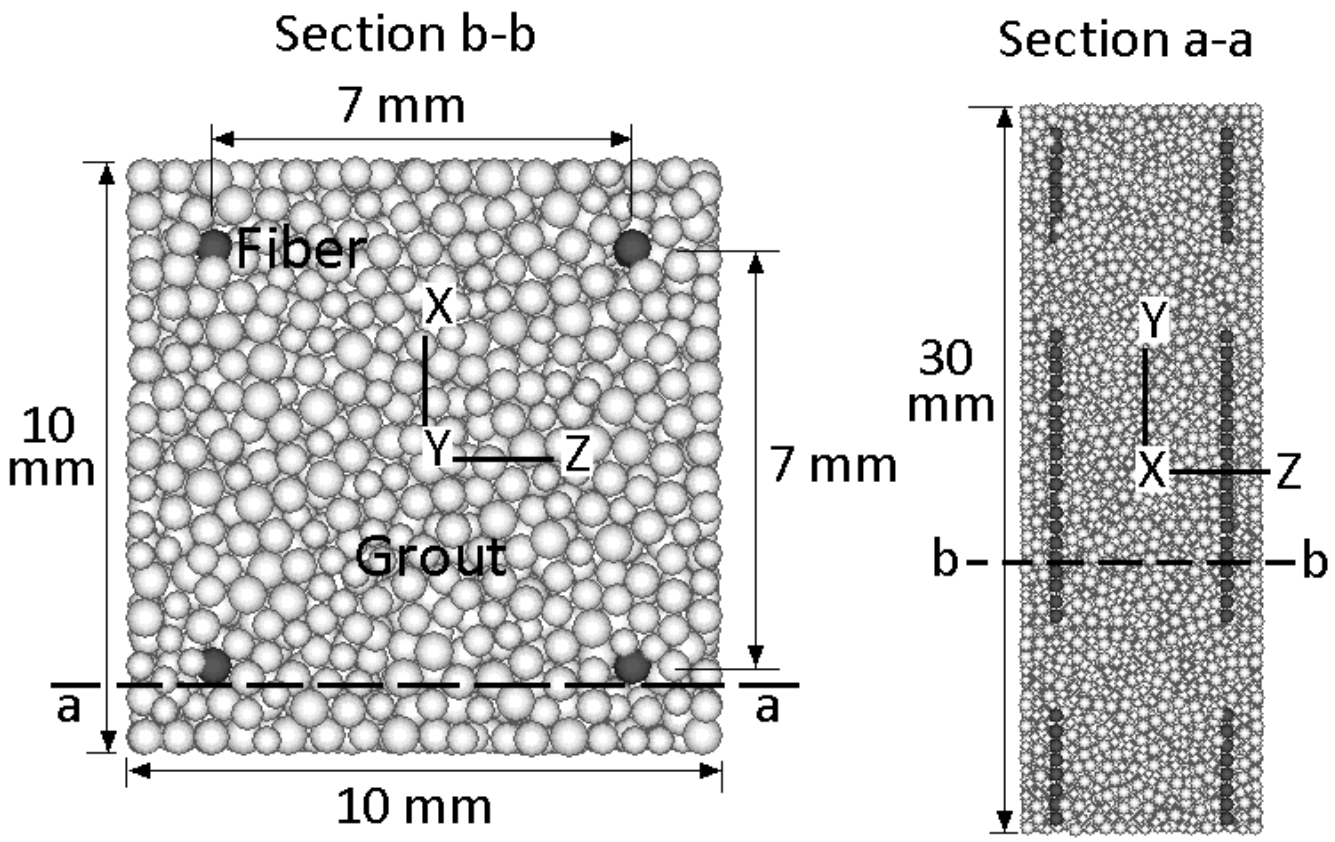

Fig. 10. DEM model of cemented grout reinforced by unidirectional fibers.

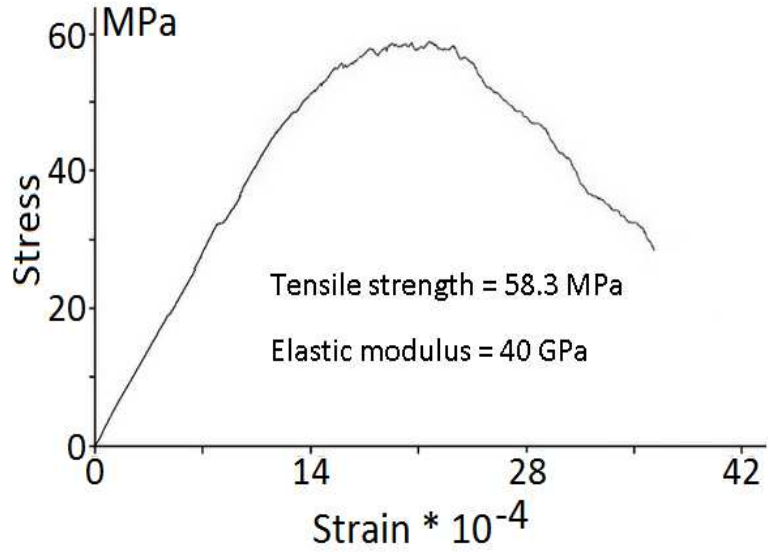

Fig. 11. Stress-strain curve of unidirectional fiber reinforced cemented grout obtained from PFC3D.

5. Conclusion

The obtained results from the experimental and DEM investigations showed that the unidirectional fibers enhanced the fracture strength of the reinforced cemented grout. However, the effect of randomly distributed fibers on the tensile strength

was not considerable. The simulation results showed that the reinforced specimens exhibited a non-linear increase of the load until the maximum load was reached, then the load gradually decreased with increasing the displacement. It illustrated that the high strain energy stored in the reinforced specimens caused a progressive fracture with pseudo plasticity behavior to occur. The cemented grout samples carry flaws and micro cracks both in the material and at the interfaces. Under an applied load, the distributed micro cracks propagate, coalesce and align themselves to produce macro cracks. When load are further increased, conditions of critical crack growth are attained at the tips of macro cracks and a catastrophic failure is precipitated. However, the fibers bridge the propagating cracks in the reinforced specimens because the grout failure precedes the fiber failure. This causes the fiber bridging zone to absorb a lot of energy by fiber debonding, fiber pullout (sliding) and fiber rupture when a crack propagates across a fiber through the grout. Consequently, the energy absorption capacity of the unidirectional fiber reinforced specimen increases and their cracking sensitivity decreases, causing the fracture strength to increase. Finally, according to the obtained results, it seems that DEM can be a suitable method for modeling tensile fracture behavior of polymer fiber reinforced cemented grouts.

REFERENCES

[1] Ahmed M. Polypropylene Fibers-Science and Technology. Amsterdam: Elsevier, 1982.

[2] Zhang S, Horrocks AR. A review of flame retardant polypropylene fibers. Prog Poly Sci 2003; 28: 1517-1538.

[3] Cengiz O, Turanli L. Comparative evaluation of steel mesh, steel fiber and high-performance polypropylene fiber reinforced shotcrete in panel test. Cem Concr Res 2004; 34 (8): 1357-1364.

[4] Singh SP. Fatigue strength of hybrid steel-polypropylene fibrous concrete beams in flexure. Proced Eng 2011; 14: 2446-2452.

[5] Song PS, Hwang S, Sheu BC. Strength properties of nylon-and polypropylene-fiber-reinforced concrete. Cem Concr Res 2005; 35 (8): 1546-1550.

[6] Hannant DJ. Durability of polypropylene fibers in Portland cement-based composites: eighteen years data. Cem Concr Res 1998; 28 (12): 1809-1817.

[7] Filho RDT, Sanjuan MA. Effect of low modulus sisal polypropylene fiber on the free and restrained shrinkage of mortars at early age. Cem Concr Res 1999; 29 (10): 1597-1604.

[8] Noumowe A. Mechanical properties and microstructure of high strength concrete containing polypropylene fibers exposed to temperatures up to 200° C. Cem Concr Res 2005; 35 (11): 2192-2198.

[9] Sun Z. Xu Q. Microscopic, physical and mechanical analysis of polypropylene fiber reinforced concrete. Mater Sci Eng A 2009; 527: 198-204.

[10] Cundall PA, Strack OD. A discrete model for granular materials. Geotech 1979; 1: 47–56.

[11] Potyondy DO, Cundall PA. A bonded-particle model for rock. Int J Rock Mec Min Sci 2004; 41: 1329–64.

[12] Jing L, Stephansson O. Fundamentals of discrete element methods for rock engineering, Theory and applications. New York: Elsevier, 2007.

[13] Refahi A, Aghazadeh Mohandesi J, Rezai B. Discrete element modeling for predicting breakage behavior and fracture energy of a single particle in a jaw crusher. Int J Miner Process 2010; 94: 83-91.

[14] Schubert W, Khanal M, Tomas J. Impact crushing of particle-particle compounds experiment and simulation. Int J Miner Process 2005; 75: 41-52.

[15] Aghazadeh Mohandesi J, Refahi A, Sadeghi Meresht E, Berenji S. Effect of temperature and particle weight fraction on mechanical and micromechanical properties of sand-polyethylene terephthalate composites: A laboratory and discrete element method study. Compos. Part B 2011; 42: 1461-1467.

[16] Akkaya Y, Peled A, Shah SP. Parameters related to fiber length and processing in cemented composites. Mater Struct 2000; 33: 515-524.

[17] Gonzalez C, Lorca J. Multiscale modeling of fracture in fiber reinforced composites. Act Mater 2006; 54: 4171-4181.

[18] Meyers MA, Chawla KK. Mechanical Behavior of Materials. New York: Cambridge University Press, 2009.

[19] Kreyszig E. Advanced Engineering Mathematics. Singapore: John Wiley & Sons, 2006.

[20] Banmthia N, Nandakumar N. Crack growth resistance of concrete reinforced with a low volume fraction of polymeric fiber. J Mater Sci Lett 2011; 20: 1651 – 1653.

[21] PFC3D. Manual of the particle flow code in 3 dimensions software. Version 2.00, Minneapolis: Itasca Consulting Group; 1999.

[22] Kawamata A, Mihashi H, Kaneko Y, Kirikoshi K. Controlling fracture toughness of grout for ductile fiber reinforced cemented composites. Eng Frac Mech 2002; 69: 249-265.

[23] Dias DP, Thaumaturgo C. Fracture toughness of geopolymeric concretes reinforced with basalt fibers. Cem Concr Comp 2005; 27: 49-54.